Chromium-Assisted Synthesis of Platinum Nanocube Electrocatalysts

Rameshwori Loukrakpam [a], Paul Chang [a], Jin Luo [a], Bin Fang [a], Derrick Mott [a], In-Tae Bae [b], H. Richard Naslund [c], Mark H. Engelhard [d], and Chuan-Jian Zhong [a]*

[a] Department of Chemistry, State University of New York at Binghamton, Binghamton, NY 13902; [b] S^3IP Analytical and Diagnostics Laboratories, Binghamton, NY 13902; [c] Department of Geology, State University of New York at Binghamton, Binghamton, NY 13902; [d] Pacific Northwest National Laboratory, Richland, WA 99352.

* To whom correspondence should be addressed. Email: cjzhong@binghamton.edu.

Electronic Support information(E.S.I.).

Experimental Section

Chemicals: Platinum (II) acetylacetonate ($Pt(acac)_2$, 97%), chromium hexacarbonyl ($Cr(CO)_6$), 99%), 1,2-hexadecanediol (90%), octyl ether (99%), and oleylamine (70%) were obtained from Aldrich. Oleic acid (99%) was obtained from Alfa Aesar. All the other solvents were of analytical grade and were used without further purification.

Synthesis of nanoparticles: (1) Synthesis of Pt nanocubes in the presence of Cr: In the modified synthesis, platinum (II) acetylacetonate (0.974 mmol) and chromium hexacarbonyl (1.004 mmol) were added to 100 ml of octyl ether followed by 2.262 mmol of 1,2-hexadecanediol, 3.136 mmol oleic acid and 2.127 mmol of oleylamine (see Supporting Information Table S1 for detailed feeding concentrations). The reaction mixture was heated under nitrogen atmosphere to a temperature of 105 °C with stirring. Nitrogen purging was stopped and the flask was sealed to prevent exposure to the atmosphere. The reaction mixture was further heated to 200 °C temperature at a rate of ~ 5 °C per min and the temperature was maintained at 200 °C for one hour. It was then cooled to room temperature. Finally, the as-synthesized dark brown colored suspension of nanoparticles was added to 200 mL ethanol and allowed to precipitate overnight. The light yellow-brown supernatant colored was removed by centrifugation at 2000 rpm for 5 min. The dark-brown sediment was re-suspended in hexane and again centrifuged. The supernatant, now purple in color was decanted and the dark-brown sediment was re-suspended in hexane. This process was repeated until the supernatant was colorless. The final nanoparticle product was suspended in fresh hexane and made ready for analysis. (2) Synthesis of Pt nanoparticles in the absence of Cr: Platinum (II) acetylacetonate (1.508 mmol) was added to 150 mL of octyl ether followed by 2.616 mmol of 1,2-hexadecanediol, 0.2851 mmol oleic acid and 6.383 mmol of oleylamine. The reaction mixture was heated under nitrogen atmosphere to a temperature of 105 °C with stirring. Nitrogen purging was stopped and the flask was sealed to prevent exposure to the atmosphere. The reaction mixture was further heated to 200 ^{0}C at a rate of ~ 5 ^{0}C/ min and the temperature was maintained at 200 ^{0}C for 15 minutes before cooling to room temperature. The dark brown colored suspension of the as-synthesized nanoparticles was added to 200 mL ethanol and allowed to precipitate overnight. The light yellow-brown supernatant was removed by centrifugation at 2000 rpm for 5 min. The dark-brown sediment was re-suspended in hexane. We also note that the synthesis of Cr nanoparticles was attempted under similar conditions but replacing the platinum acetylacetonate precursor with chromium hexacarbonyl precursor, which did not yield Cr nanoparticles.

Preparation of catalysts and electrodes: The electrocatalysts were prepared by loading the as-synthesized Pt nanoparticles and Pt nanocubes on carbon black (Vulcan-72). Carbon black was pretreated at 900 ^{0}C under nitrogen for 120 min. In a typical experiment, 150 mg of carbon black was suspended in 150 mL of hexane. This suspension was sonicated for 3 hours in a ice

bath. The nanoparticles were added to the suspension with ~20 % by weight metal loading and sonicated for 1 hour. The suspension was stirred for ~16 hours. It was centrifuged at 5000 rpm for 5 min to separate the solvent. The powders collected from this process were treated in a programmable furnace in nitrogen atmosphere at 280 ^{0}C for 60 minutes and then with a mixture of 10% oxygen and 90% nitrogen atmosphere at 280 ^{0}C for 30 min to activate the catalyst, which involved removal of the organic shell from the nanoparticle core and calcination of the catalyst. The catalysts were also calcined at 280 ^{0}C in hydrogen atmosphere for 30 min. The metal loading of the nanoparticles on carbon support was determined by thermogravimetric analysis.Details of the preparation protocols were documented in earlier reports.

Glassy carbon (GC) electrodes (geometric area: 0.196 cm^2) were polished with 0.03 μm Al_2O_3 powders, followed by careful rinsing with deionized water. A typical suspension of the catalysts was prepared by suspending 5 mg catalysts in 4 mL Millipore water with 20 μL diluted of (5% vol.) Nafion^{TM} (5 wt%, Aldrich). The suspension was ultrasonicated at 20% amplitude for 10 min and then quantitatively transferred to the surface of the polished GC disk.

Instrumentation and Measurements: The nanoparticles and catalysts were characterized using Thermogravimetric Analysis (TGA), Transmission Electron Microscopy (TEM), High-Resolution Transmission Electron Microscopy–Energy Dispersive X-ray Spectroscopy (HRTEM-EDS), Direct Current Plasma–Atomic Emission Spectrometers (DCP-AES), X-ray Photoelectron Spectroscopy (XPS), X-ray powder diffraction (XRD), and electrochemical measurments.

The composition was analyzed using the DCP-AES technique, which was performed on an ARL Fisons SS-7 Direct Current Plasma-Atomic Emission Spectrometer. The nanoparticle samples were dissolved in concentrated aqua regia, and then diluted to concentrations in the range of 1 to 50 ppm for analysis. Calibration curves were made from dissolved standards with concentrations from 0 to 50 ppm in the same acid matrix as the unknowns.

TGA was performed on a Perkin-Elmer Pyris 1-TGA for determining of the concentration of nanoparticles in hexane suspension, amount of capping agents and for metal loading. Typical samples weighed ~4 mg and were heated in a platinum pan.

TEM was done on a Hitachi H-7000 electron microscope (100kV). HRTEM-EDS was carried out using a JEOL JEM 2010F at an acceleration voltage of 200kV. The nanoparticles were diluted in hexane, and drop cast onto a carbon-coated copper grid, followed by solvent evaporation in air at room temperature.

XRD data was collected from 20 to 90 degree 2θ at a rate of 0.58 degrees/min at room temperature on a Scintag XDS2000 θ - θ diffractometer using Cu Kα λ= 1.5418 Å, equipped with a Ge (Li) solid state detector. The diffraction data was compared to the XRD database of International Centre for Diffraction Data.

XPS measurements were collected using a Physical Electronics Quantum 2000 Scanning ESCA Microprobe. This system uses a focused monochromatic Al K_α x-ray (1486.7 eV) source and a spherical section analyzer. The instrument has a 16 element multichannel detector. The X-ray beam used was a 100 W, 100 μm diameter that was rastered over a 1.3 mm by 0.2 mm rectangle on the sample. The X-ray beam was incident normal to the sample and the photoelectron detector was at 45° off-normal. Wide scan data was collected using pass energy of 117.4 eV. For the Ag $3d_{5/2}$ line, these conditions produce FWHM of better than 1.6 eV. High-energy resolution photoemission spectra were collected using pass energy of 46.95. For the Ag $3d_{5/2}$ line, these conditions produced FWHM of better than 0.77 eV. The binding energy (BE) scale was calibrated using the Cu $2p_{3/2}$ feature at 932.62 ± 0.05 eV and Au 4f at 83.96 ± 0.05 eV for known standards. The sample experienced variable degrees of charging. The vacuum chamber pressure during analysis was < $1.3x10^{-6}$ Pa. Samples were drop casted onto a molybdenum substrate and were allowed to dry. The C 1s peak was used as an internal standard (284.9 eV) for the calibration of the binding energy.

Electrochemical measurements such as cyclic voltammetric (CV) and rotating disk electrode (RDE) measurements were performed using a computer-controlled electrochemical

analyzer (CHI 600A). The experiments were performed in a three-electrode cell at room temperature using 0.1 M $HClO_4$ as electrolyte, which was deaerated with high-purity nitrogen for CV measurements, or saturated with oxygen for rotating disk electrode measurements. The potentials are given with respect to reversible hydrogen electrode (RHE). Both CV and RDE curves were obtained from least 3 times of repetitive measurements, and the ECA, MA and SA values were reproducible within 10% error bar usually observed for this type of electrochemical systems.

Results and Discussion

This reaction led to the formation of nanoparticles which could be re-suspended in hexane, and a supernatant that remained purple-colored with two peaks at 425 and 555 nm in UV-Vis spectra irrespective of the feeding ratio used. These two peaks were characteristic of transitions of Cr (III) ions ($4A_{2g}\rightarrow 4T_{2g}$ and $2A_{2g}\rightarrow 2T_{1g}$, $2E_{2g}$), [50] indicating that the Cr precursors remained basically in the solution as Cr (III) after the completion of the reaction.

In addition to the uniform shape and size, the presence of the capping molecules on the nanocrystals was essential for the formation of the ordered domains. The TGA analysis of the organic vs. metal mass ratio in the nanoparticle product showed a mass of 8~9% for the organic capping molecules. Theoretically, the percentage of mass of the organic shells on the nanoparticles for a 7.0-nm cubic Pt nanoparticle (~22,720 Pt atoms, and ~1470 capping oleylamine and oleic acid molecules) is estimated to be 8.3% for full monolayer coverage, which is very close to the experimentally determined value.

The nanoparticles synthesized from a lower Pt:Cr precursor ratio, e.g., 1:3, showed cubic morphology similar to those synthesized with a precursor ratio of 1:1 (Figure S1(a)), but the average particle size was increased with a lower monodispersity (11.0 ± 1.9 nm). The decreased monodispersity was as evidenced by the lack of ordered domains in comparison with those synthesized with a feeding ratio of 1:1. However, attempts with a higher Pt:Cr precursor ratio, e.g., 3:1, led to a mixture of nanoparticles of different sizes and shapes (Figure S1(b)). In this case, a wide range of shapes such as sphere, triangles, and irregular cubes can be observed with a very broad size distribution from 2 to 30 nm.

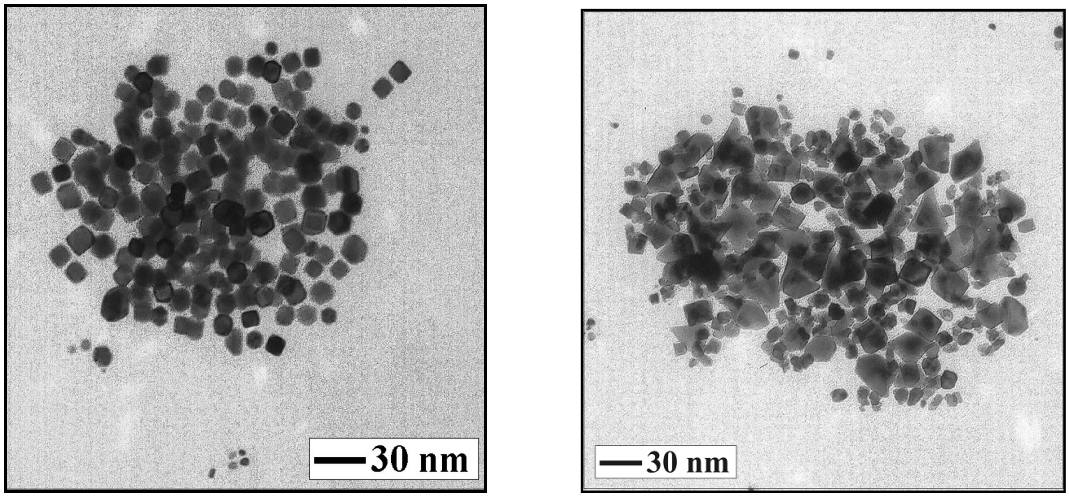

(a) (b)

Figure S1. *TEM micrographs and size distributions (diameter, d) of the nanoparticles synthesized from different Pt:Cr feeding ratios: 1:3 (b,11.0 ± 1.9 nm) and 3:1 (c)*

Table S1. Detailed synthetic feeding of Pt- and Cr-precursors

Pt:Cr (atomic ratio)	Pt (mM)	Cr(mM)
1:3	4.9	14.7
1:1	8.2	8.2
3:1	14.7	4.9

The composition of the nanocubes was further analyzed using surface-sensitive XPS technique. Figure S2 shows a representative set of XPS spectra in the binding energy regions of Pt 4f (a) and Cr 2p (b). Pt $4f_{7/2}$ and $4f_{5/2}$ bands were clearly identified at 70.3 and 73.7 eV, respectively. In the Cr 2p region, the doublet peaks (Cr $2p_{3/2}$ and $2p_{1/2}$) expected for Cr species [51] were barely detected at ~577 and ~586 eV above the background. It is interesting to note that the binding energies for the observed Pt $4f_{7/2}$ and $4f_{5/2}$ bands displayed a shift (~0.8 eV) to lower energies in comparison with those for Pt^0 (71.0 ~71.2 for $4f_{7/2}$ and 74.3 ~ 74.5 for $4f_{5/2}$) [52,53]. This finding implies an increased electron density on the surface of the Pt nanocrystals. While the exact origin of the binding energy shift will need a further investigation, the –0.8 eV shift may reflect partly a charge transfer from the encapsulating oleic acid and oleylamine monolayer to the Pt nanocrystal surface. This assessment is based on the fact that a similar shift in Pt 4f bands is recently reported for Pt nanoparticles of 2 ~ 7 nm sizes capped with polyvinylpyrolidone (PVP) in which a charge transfer from PVP (electron donor) to Pt (electron acceptor) was proposed to create a higher electron density at Pt which was responsible for the lower Pt 4f binding energy (Pt $4f_{7/2}$ ~70.6 eV) [52, 53]. This type of electronic effect was shown to be size-dependent [53], and was also confirmed for other capped metal nanoparticles such as gold [54]. The XPS composition analysis showed a average atomic ratio of 88:12 (Pt:Cr) with ±1% error . Considering a depth profile of ~5 nm and an attenuation effect in XPS analysis, a rough estimate of the relative composition based on an idealized model for the 7 nm sized nanocube yielded about ~1% Cr, most of which is likely concentrated on the surface.

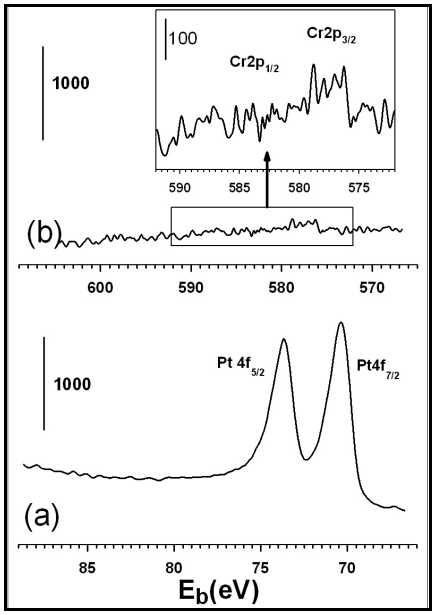

Figure S2. *XPS spectra of the as-synthesized nanocubes in the binding energy regions of Pt 4f (a) and Cr 2p (b)*

The bulk composition of the as-synthesized nanocubes was further determined using DCP-AES and EDS techniques. The DCP-AES analysis of the nanoparticles synthesized with all feeding ratios of Pt:Cr showed a composition of 99% Pt and 1% Cr (±2%). This bulk analysis result was found to be practically the same as the composition values obtained from the EDS analysis, which gave a composition of 99% Pt and 1% Cr (±1%) in the nanocubes. All these analytical results indicated that practically there was no Cr in the Pt nanocubes or only a trace of Cr on the nanocrystal surfaces considering the error sizes (1~2%) for these techniques. The inability for Cr to form the alloy nanoparticles under this experimental condition was likely due to ineffective reduction and easy re-oxidation of Cr in this system as discussed in the next subsection. The Cr-assisted synthesis strategy is shown to be highly effective in producing Pt nanocubes.

The presence of Cr in the nanocubes was further assessed by a comparison of the EDX-determined composition data between the as-synthesized nanocubes and the carbon-supported catalysts after thermal treatment (Figure S3). In contrast to the detectable Cr for the as-synthesized nanocubes, which gave a composition of 99.2% Pt and 0.8% Cr (±1%), Cr was not detected for the carbon-supported catalysts within the detection limit of the measurement. While the exact fate of Cr is still under investigation, possible reasons include that Cr was washed away from the nanocrystal surface with the solvents during the asembly process, that the Cr present on the surface was below the detection limit (0.4~1%), and that Cr was removed during the thermal treatment as a result of a possible reduced sublimation temperature[56]. As such, the surface composition of the carbon-supported nanocubes after the thermal treatment can be considered to be consisting of either pure Pt or a surface layer of PtCr alloy.

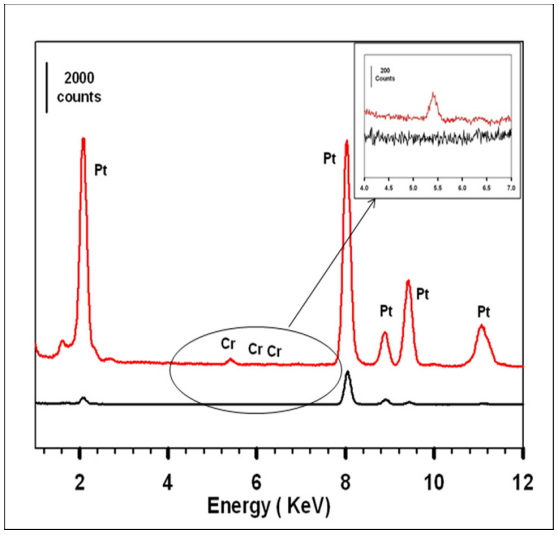

Figure S3. *EDS spectra of as-synthesized nanocubes before (top curve) and after (bottom curve) thermal treatment. Insert: a magnified view of the energy region for Cr. The Cr region has been normalized using the Pt 8.0 KeV peak.*

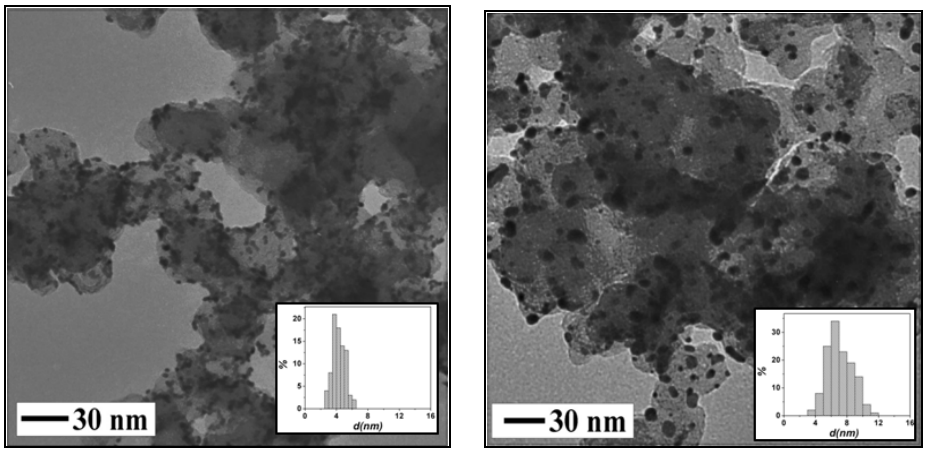

(a) **(b)**

Figure S4. TEM micrograph of Pt-nanoparticle/C before (a, 4.3± 0.8 nm) and after (b, 7.1± 1.6 nm) thermal treatment.

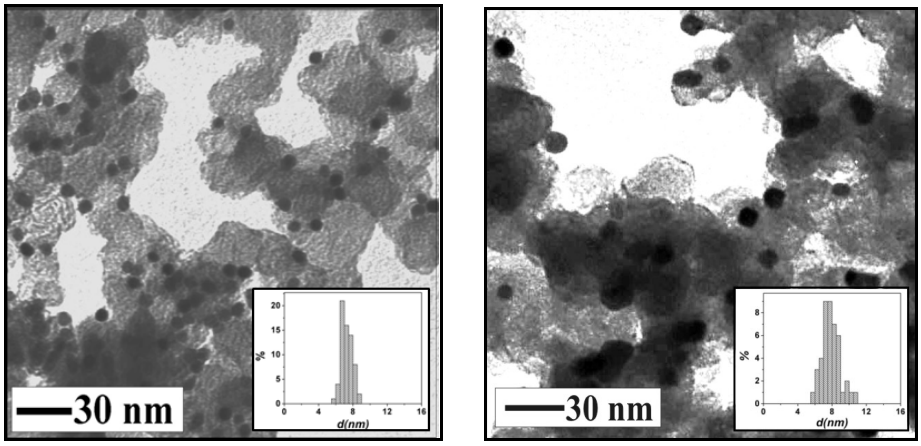

(a) **(b)**

Figure S5. TEM micrograph of Pt-nanocube/C before (a, 7.2± 0.6 nm) and after (b, 7.9± 1.1 nm) thermal treatment.

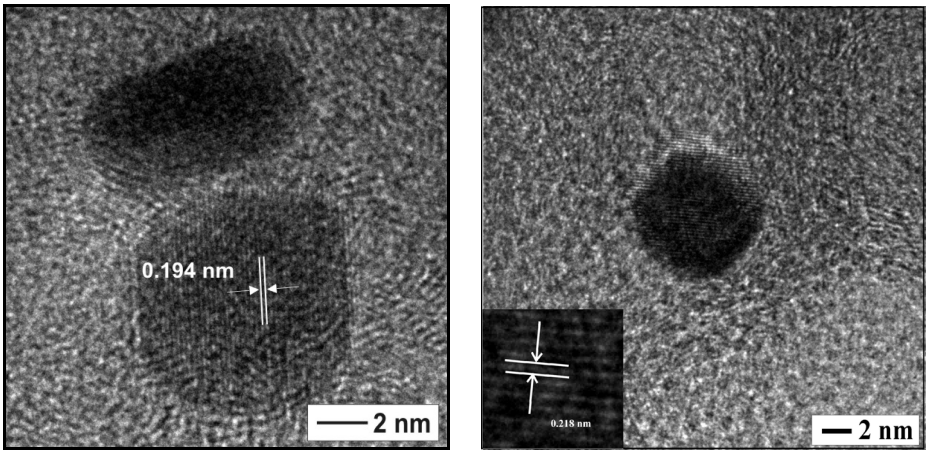

(a) (b)

Figure S6. HRTEM of Pt-nanocube/C on carbon: (a) observation of lattice fringes corresponding to (100) plane of nanocubes (b) observation of lattice fringes corresponding to (111) plane at trancated corner of the nanocube.

References:

[SI-1] H. Xu, T. Lou, Y. Li, *Inorg. Chem. Comm*., 2004, **7**, 666.

[SI-2] M. Aronniemi, J. Sainio, J. Lahtinen, *Surface Science,* 2005, **578***,* 108.

[SI-3] X. Fu, Y. Wang, N. Wu, L. Gui, Y. Tang, *J. Colloid Interface Sci.,* 2001, **243**, 326.

[SI-4] L. Qiu, F. Li, L. Zhao, W. Yang, J. Yao, *Langmuir*, 2006, **22**, 4480.

[SI-5] H. Tsunoyama, N. Ichikuni, H. Sakurai, T. Tsukuda, *J. Am. Chem. Soc*., 2009, **131**, 7086.

[SI-6] H. H. Farrell et al. The 20th North American Catalysis Society Meeting, Houston, TX, June 17-22, 2007.